Decoherence and disentanglement scenarios in non-Markovian quantum Brownian motion

2008 J. Phys. A: Math. Theor. 41 265301

(http://iopscience.iop.org/1751-8121/41/26/265301)

IOP PUBLISHING JOURNAL OF PHYSICS A: MATHEMATICAL AND THEORETICAL

J. Phys. A: Math. Theor. **41** (2008) 265301 (15pp) doi:10.1088/1751-8113/41/26/265301

Decoherence and disentanglement scenarios in non-Markovian quantum Brownian motion

C Hörhammer and H Büttner

Theoretische Physik I, Universität Bayreuth, D-95440 Bayreuth, Germany

E-mail: christian.hoerhammer@uni-bayreuth.de

Received 11 December 2007, in final form 25 March 2008
Published 11 June 2008
Online at stacks.iop.org/JPhysA/41/265301

Abstract

We study the non-Markovian decoherence and disentanglement dynamics of dissipative quantum systems with special emphasis on non-Gaussian continuous variable systems. The dynamics are described by the Hu–Paz–Zhang master equation of quantum Brownian motion. The time evolution of the decoherence function of a single-mode superposition is compared to the concurrence of a two-mode entangled state. It is verified that moderate non-Markovian influences slow down the decay of interference fringes and quantum correlations, while strong non-Markovian effects resulting from an out-of-resonance bath can even accelerate the loss of coherence, compared to predictions of Markovian approximations. Qualitatively different scenarios including exponential, Gaussian or algebraic decay of the decoherence function are analyzed. It is shown that partial revivals of coherence can occur in case of non-Lindblad-type dynamics.

PACS numbers: 05.40.−a, 03.65.Yz, 03.67.−a

(Some figures in this article are in colour only in the electronic version)

1. Introduction

During the last decade quantum information and computation has been extended from discrete systems to quantum systems with continuous variables such as position and momentum or the amplitudes of electromagnetic field modes. This quantum information theory of continuous variable systems has received much attention in the past few years [1–3] and has found various applications in quantum cryptography and quantum teleportation [4, 5]. Great advances have been made in characterizing the entanglement properties of two-mode Gaussian states by determining the necessary and sufficient criteria for their separability [6, 7] and by developing quantitative entanglement measures [8, 9]. Non-Gaussian continuous variable states are more difficult to treat theoretically and to be controlled experimentally. Therefore they got much

less attention in recent years. However, especially the class of entangled coherent states offers the possibility of applying concepts such as concurrence, first developed for discrete systems and of studying the non-Markovian disentanglement dynamics of these states.

Due to the unavoidable interaction with the environment, any pure quantum state used in quantum information processing evolves into a mixed state. Thus, a realistic analysis of continuous variable quantum channels must take decoherence and dissipation into account. Decoherence describes the environment-induced suppression of the quantum-mechanical coherence properties and interference ability. This concept is strongly related to the measurement problem [10–13] and the transition from the quantum to the classical regime [14–18]. The time scales on which these processes take place and strategies to reduce these effects are a major topic of research. Thereby, the theoretical results strongly depend on the underlying dissipative dynamics and the performed approximations.

Within the theory of open quantum systems [19, 20] the dissipative dynamics are mainly described by master equations of the reduced density matrix. Initial quantum superpositions are destroyed and quantum correlations are lost during characteristic decoherence and separability time scales. The Markovian time evolution of quantum correlations of entangled two-mode continuous variable states has been examined in single-reservoir [21, 22] and two-reservoir models [7, 17, 23, 24], representing noisy correlated or uncorrelated Markovian quantum channels. Quantum correlations are found to be better preserved in a common reservoir. Additionally, the coupling to the same bath variables might generate new quantum correlations between the parts of the subsystem. This effect of environment-induced entanglement has already been studied for discrete systems [22, 25, 26] and can lead to asymptotically entangled states [27–30]. The underlying Born-Markov approximation assumes weak coupling between the system and the environment to justify a perturbative treatment and neglects short-time correlations between the system and the reservoir. This approach has been widely and successfully employed in the field of quantum optics [31] where the characteristic time scales of the environmental correlations are much shorter compared to the internal system dynamics. Challenged by new experimental evidence a growing interest in non-Markovian descriptions can be observed. Very recently some phenomenological [32, 33] and microscopic models [34–37] of non-Markovian quantum channels have been proposed. Using the analogy between the Hilbert space of quantized electromagnetic fields and the Hilbert space of quantum harmonic oscillators, the Caldeira–Leggett model of quantum Brownian motion [38–40] can be extended to describe the entanglement dynamics of two-mode squeezed states.

Non-Markovian effects on decoherence and disentanglement dynamics become important if the decoherence time scale τ_d (i.e. the time during which interference terms in the initial density matrix/Wigner function disappear) and the bath correlation time scales τ_b (i.e. autocorrelation time of noise kernel) are comparable. This might be the case for macroscopic superposition since the decoherence time is reduced for increased separation in phase space. The explicit course of the decoherence process depends on the relation of the characteristic time scales of system τ_s (i.e. the oscillation period) and environment τ_b on one hand and the decoherence time scale τ_d on the other hand. Depending on the relation of the characteristic time scales — including the relaxation time scale τ_γ (i.e. the time during which an arbitrary initial density matrix/Wigner function evolves into that of a canonical state) — four different regimes can be distinguished:

$$\tau_b \ll \tau_s \ll \tau_\gamma \qquad \text{Born–Markovian regime,} \tag{1}$$

$$\tau_b \approx \tau_s \ll \tau_\gamma \qquad \text{Non-Markovian regime,} \tag{2}$$

$$\tau_b \ll \tau_s \approx \tau_\gamma \qquad \text{Strong-coupling regime,} \tag{3}$$

$$\tau_s < \tau_b \ll \tau_\gamma \qquad \text{Out-of-resonance regime.} \tag{4}$$

Since the decoherence time of superposed coherent states depends on the phase-space separation, the initial preparation mainly determines the ratio of the decoherence time to the other characteristic time scales. We will focus on the non-Markovian regime where different decoherence scenarios exist — for both, the dynamics of single-mode superpositions as well as the disentanglement of two-mode entangled coherent states.

The paper is organized as follows. In section 2, we briefly review the properties of entangled coherent states as a special class of non-Gaussian continuous variable states and introduce relevant decoherence and entanglement measures. In section 3, we describe the Hu–Paz–Zhang (HPZ) master equation of quantum Brownian motion which is the basis for studying non-Markvoian effects. We resume the extended, two-mode version of the Caldeira–Leggett model for single and two-reservoir models. In section 4, we present and discuss the numerical results of the decoherence and entanglement dynamics of a single-mode superposed coherent state compared to a two-mode entangled coherent state. Different scenarios are analyzed, including exponential, Gaussian and algebraic decay as well as revivals of decoherence. It is shown that the behavior of the concurrence of an entangled two-mode state is equivalent to the behavior of the decoherence function of a single-mode superposition state. Finally, a brief summary is given in section 5.

2. Non-Gaussian continuous variable states

2.1. Entangled coherent states (ECS)

In the following we consider entangled coherent states [41, 42] as a special class of non-Gaussian continuous variable states. An example of a multi-mode entangled coherent state is given by

$$|\alpha,\theta,N\rangle = \frac{|\alpha_+\rangle_1 \otimes |\alpha_+\rangle_2 \otimes \ldots \otimes |\alpha_+\rangle_N + \mathrm{e}^{\mathrm{i}\theta}|\alpha_-\rangle_1 \otimes |\alpha_-\rangle_2 \otimes \ldots \otimes |\alpha_-\rangle_N}{\sqrt{2+2\,\mathrm{e}^{-2N|\alpha_0|^2}\cos\theta}}, \tag{5}$$

which is a superposition of coherent states $|\alpha_\pm\rangle_i = \hat{D}(\pm\alpha_0)|0\rangle_i$ with displacement parameter $|\alpha_0|^2 = \frac{q_0^2}{4\sigma_0^2} + \frac{\sigma_0^2 p_0^2}{\hbar^2}$ and σ_0 as the width of a minimum uncertainty wave packet displaced at q_0, p_0 (mean values) in phase space. In particular, we will focus on the two-mode version

$$|\Phi_\pm\rangle := |\alpha,\theta=\{0,\pi\},N=2\rangle = \frac{(|\alpha_+\rangle_1|\alpha_+\rangle_2 \pm |\alpha_-\rangle_1|\alpha_-\rangle_2)}{\sqrt{2(1\pm\mathrm{e}^{-4|\alpha_0|^2})}} \tag{6}$$

which is also known as quasi-Bell state [35, 43, 44] due to its similarity to the well-known Bell states as maximally entangled two-qubit states. In addition to a violation of the Bell inequalities [45] these states show further nonclassical properties, such as sub-Poissonian statistics, squeezing and a violation of the Cauchy–Schwarz inequaltiy [46]. Contrary to entangled single Fock states [47] ECS are superpositions of non-orthogonal states [48] with some remarkable properties [49–51].

If just a single mode is considered, we get the well-known cat-state superposition of two coherent states

$$|\psi_\alpha\rangle = \frac{|\alpha_+\rangle + \mathrm{e}^{\mathrm{i}\theta}|\alpha_-\rangle}{\sqrt{2+2\,\mathrm{e}^{-2|\alpha_0|^2}\cos\theta}} \tag{7}$$

(which is of course not entangled). Its density matrix can be separated into two parts,

$$\rho_\alpha(0) = \underbrace{\frac{|\alpha_+\rangle\langle\alpha_+| + |\alpha_-\rangle\langle\alpha_-|}{2(1+\mathrm{e}^{-2|\alpha_0|^2})}}_{\rho_{cl}(0)} + \underbrace{\frac{|\alpha_-\rangle\langle\alpha_+| + |\alpha_+\rangle\langle\alpha_-|}{2(1+\mathrm{e}^{-2|\alpha_0|^2})}}_{\rho_I(0)}, \tag{8}$$

a classical part ρ_{cl} and a part ρ_I describing the quantum-mechanical ability to interfere (here $\theta = 0$). The corresponding phase-space representation in the form of the Wigner function

$$W_{\pm q_0}(q, p, 0) = \frac{\mathrm{e}^{-q^2/2\sigma_0^2 - 2p^2\sigma_0^2/\hbar^2}}{\pi\hbar(1 + \mathrm{e}^{q_0^2/2\sigma_0^2})} \left(\mathrm{e}^{q_0^2/2\sigma_0^2} \cos\frac{2q_0 p}{\hbar} + \cosh\frac{q_0 q}{\sigma_0^2} \right), \tag{9}$$

(for $|\alpha_0|^2 = \frac{q_0^2}{4\sigma_0^2}$) has two characteristic peaks at $q = \pm q_0$ and an oscillating pattern in between with partially negative values of the Wigner function. It is one of the most common examples for studying decoherence for continuous variable states. In this paper, we want to compare the decoherence properties of these states within a non-Markovian description to the disentanglement process of a two-mode entangled coherent state.

2.2. Decoherence and disentanglement measures

2.2.1. Decoherence of a single-mode superposition state. There are different measures of decoherence in phase space, in position and momentum space or Fock space representation. Decoherence time scales based on different measures can deviate from each other. In our view, phase-space measures give the better picture of the underlying non-Markovian process compared to a treatment in position space alone (i.e. the so-called attenuation factor or the fringe visibility function). Decoherence in phase space can be described by the time evolution of the purity $\mu(t) = \mathrm{Tr}[\rho^2(t)]$ or the so-called quantumness $\Xi(t) = \int \mathrm{d}q\, \mathrm{d}p |W(q, p, t)| - 1$ which measures the phase-space volume of the negative part of the Wigner function. While the first mixes decoherence and relaxation phenomena and the latter is difficult to calculate, the norm $\mu_I(t) = \mathrm{Tr}\left[\rho_I^2(t)\right]$ of the interference part seems to be an adequate measure for decoherence [52]. It can be calculated from the oscillating part $W_I(q, p, t)$ of the Wigner function by

$$\mu_I(t) = (2\pi\hbar)^2 \int_{-\infty}^{\infty} \mathrm{d}q \int_{-\infty}^{\infty} \mathrm{d}p W_I^2(q, p, t). \tag{10}$$

The non-Markovian time evolution of the Wigner function is governed by a quantum Fokker–Planck equation given in the third section.

2.2.2. Disentanglement of a two-mode entangled coherent state. To study the entanglement properties of a non-Gaussian continuous variable state we use the concept of concurrence [53, 54]. For the density matrix ρ_{12} of a pair of qubits the concurrence is defined as $\mathcal{C}_{12} = \max\{\lambda_1 - \lambda_2 - \lambda_3 - \lambda_4, 0\}$, where $\lambda_1 \geqslant \lambda_2 \geqslant \lambda_3 \geqslant \lambda_4$ are the square roots of the eigenvalues of the spin-flipped state $\varrho_{12} \equiv \rho_{12}(\sigma_y \otimes \sigma_y)\rho_{12}^*(\sigma_y \otimes \sigma_y)$ with Pauli matrix σ_y. The concurrence varies from $\mathcal{C}_{12} = 0$ for disentangled qubits 1 and 2 to $\mathcal{C}_{12} = 1$ for maximally entangled states. To determine the pairwise entanglement of an N-mode system in analogy to the discrete N-qubit system the reduced density matrix $\rho_{12} = \mathrm{Tr}_{2,4,..,N}\{|\alpha, \theta, N\rangle\langle\alpha, \theta, N|\}$ of two modes 1 and 2 has to be considered (all reduced density matrices ρ_{kl} of any two modes k and l are identical). The trick is to represent the density matrix

$$\begin{aligned}\rho_{12} = \frac{1}{2(1 + \mathrm{e}^{-4N|\alpha|^2})} \{ & |\alpha_+\rangle|\alpha_-\rangle\langle\alpha_+|\langle\alpha_-| + |\alpha_-\rangle|\alpha_+\rangle\langle\alpha_-|\langle\alpha_+| \\ & + \mathrm{e}^{\mathrm{i}\theta - 2(N-2)|\alpha|^2} |\alpha_-\rangle|\alpha_+\rangle\langle\alpha_+|\langle\alpha_-| + \mathrm{e}^{-\mathrm{i}\theta - 2(N-2)|\alpha|^2} |\alpha_+\rangle|\alpha_-\rangle\langle\alpha_-|\langle\alpha_+| \}\end{aligned} \tag{11}$$

in an orthogonal basis $\{|\mathbf{0}\rangle, |\mathbf{1}\rangle\}$ with $|\mathbf{0}\rangle \equiv |\alpha_+\rangle$ and $|\mathbf{1}\rangle \equiv \frac{|\alpha_-\rangle - \mathrm{e}^{-2|\alpha|^2}|\alpha_+\rangle}{\sqrt{1-\mathrm{e}^{-4|\alpha|^2}}}$,

$$\rho_{12} = N_0^2 \begin{pmatrix} 2p^2(1+q\cos\theta) & pM(1+q\,\mathrm{e}^{\mathrm{i}\theta}) & pM(1+q\,\mathrm{e}^{-\mathrm{i}\theta}) & 0 \\ pM(1+q\,\mathrm{e}^{-\mathrm{i}\theta}) & M^2 & M^2 q\,\mathrm{e}^{-\mathrm{i}\theta} & 0 \\ pM(1+q\,\mathrm{e}^{\mathrm{i}\theta}) & M^2 q\,\mathrm{e}^{\mathrm{i}\theta} & M^2 & 0 \\ 0 & 0 & 0 & 0 \end{pmatrix} \tag{12}$$

with parameters $p = \mathrm{e}^{-2|\alpha|^2}$, $N_0 = (2+2p^N\cos\theta)^{-1}$, $q = p^{N-2}$ and $M = \sqrt{1-p^2}$ [42]. By determining the four eigenvalues $\lambda_1 = N_0^2M^2(1+q)$, $\lambda_2 = N_0^2M^2(1-q)$ and $\lambda_3 = \lambda_4 = 0$ the concurrence of the reduced state ρ_{12} can be calculated to

$$\mathcal{C}_{12} = \frac{M^2 q}{1+p^N\cos\theta} = \frac{\mathrm{e}^{-2N|\alpha|^2}(1-\mathrm{e}^{4|\alpha|^2})}{1+\mathrm{e}^{-2N|\alpha|^2}\cos\theta}. \tag{13}$$

In case of a two-mode state ($N = 2$) we have pure state entanglement. The entanglement dynamics are then described by the time evolution of the parameters $p(t), q(t)$ and $M(t)$. A specific model will be introduced in the following section.

3. Non-Markovian dynamics of continuous variable states

3.1. HPZ master equation of quantum Brownian motion

Non-Markovian effects are discussed here on the basis of the Caldeira–Leggett model of quantum Brownian motion [38, 55, 56] often referred to as the independent-oscillator-model [39, 57]. It is a system plus reservoir model where the total Hamiltonian $H = H_s + H_b + H_{\mathrm{int}}$ consists of three parts, with H_s as Hamiltonian of the subsystem which interacts via the Hamiltonian H_{int} with a bath that is described by a collection of a large number of harmonic oscillators $H_b = \sum_i \hbar\omega_i(b^\dagger b + 1)$. In detail the Hamiltonian of the Caldeira–Leggett model is given by

$$H = \frac{p^2}{2m} + V(q) + \sum_{i=1}^{N}\left[\frac{p_i^2}{2m_i} + \frac{m_i\omega_i^2}{2}\left(x_i - \frac{c_i q}{m_i\omega_i^2}\right)^2\right], \tag{14}$$

where q and p are the Heisenberg operators of coordinate and momenta of the Brownian oscillator moving in a harmonic potential $V(q) = \frac{1}{2}m\omega_0^2q^2$ and coupled to a bath of N independent harmonic oscillators with variables x_i, p_i and frequencies ω_i. The bath is characterized by its spectral density

$$J(\omega) = \pi\sum_{i=1}^{N}\frac{c_i^2}{2m\omega_i}\delta(\omega-\omega_i) = \frac{\gamma\omega\Gamma^2}{\omega^2+\Gamma^2}. \tag{15}$$

The interaction is bilinear in the coordinates q and x_i of the subsystem and the bath respectively with coupling parameters c_i. The self-interaction term (proportional to q^2) in the Hamiltonian

$$H_{\mathrm{int}} = \sum_i\left[-c_i x_i q + \frac{c_i^2}{2m_i\omega_i^2}q^2\right] \tag{16}$$

renormalizes the oscillator potential to ensure that the observable frequency is close to bare oscillator frequency ω_0. From influence functional path integral techniques Hu, Paz, Zhang have derived the master equation

$$\dot\rho = \frac{1}{\mathrm{i}\hbar}[H_s,\rho] + \frac{m\delta\Omega^2(t)}{2\mathrm{i}\hbar}[q^2,\rho] + \frac{\gamma_p(t)}{2\mathrm{i}\hbar}[q,\{p,\rho\}] + \frac{D_{qp}(t)}{\hbar^2}[q,[p,\rho]] - \frac{D_p(t)}{\hbar^2}[q,[q,\rho]], \tag{17}$$

with $[\cdot]$ and $\{\cdot\}$ denoting commutator and anti-commutator respectively. This master equation is valid for arbitrary coupling and temperature. The non-Markovian character is contained in the time-dependent coefficients which read in expansion up to the second order in the system-bath coupling constant [40]:

$$\gamma_p(t) = \frac{2}{\hbar m\omega_0}\int_0^t \mathrm{d}t' L(t')\sin\omega_0 t' \overset{t\gg\Gamma^{-1}}{\longrightarrow} \frac{\gamma}{m}\frac{\Gamma^2}{\omega_0^2+\Gamma^2}, \tag{18}$$

$$\delta\Omega^2(t) = \frac{\gamma\Gamma}{m} - \frac{2}{\hbar m}\int_0^t \mathrm{d}t' L(t')\cos\omega_0 t' \overset{t\gg\Gamma^{-1}}{\longrightarrow} \frac{\gamma\Gamma}{m}\left(1-\frac{\Gamma^2}{\omega_0^2+\Gamma^2}\right), \tag{19}$$

$$D_{qp}(t) = \frac{1}{m\omega_0}\int_0^t \mathrm{d}t' K(t')\sin\omega_0 t' \overset{t\gg\Gamma^{-1}}{\longrightarrow} m\gamma_q(\infty)\langle q^2\rangle - \frac{\langle p^2\rangle}{m}, \tag{20}$$

$$D_p(t) = \int_0^t \mathrm{d}t' K(t')\cos\omega_0 t' \overset{t\gg\Gamma^{-1}}{\longrightarrow} \langle p^2\rangle\gamma_p(\infty), \tag{21}$$

where $L(t) = \mathrm{i}\langle[\eta(t),\eta(0)]\rangle$ and $K(t) = \frac{1}{2}\langle\{\eta(t),\eta(0)\}\rangle$ are connected to the spectral density (15) by

$$L(t) = \frac{\hbar}{\pi}\int_0^\infty \mathrm{d}\omega J(\omega)\sin\omega t, \tag{22}$$

$$K(t) = \frac{\hbar}{\pi}\int_0^\infty \mathrm{d}\omega J(\omega)\coth\left(\frac{1}{2}\beta\hbar\omega\right)\cos\omega t. \tag{23}$$

$K(t)$ is the correlation function of the quantum noise term η resulting from averaging over the initial thermal bath distribution. In the following the stationary values of the HPZ coefficients given in equations (18)–(21) for $t \gg \Gamma^{-1}$ will be used as coefficients in the corresponding Markovian master equations as a basis for comparison. The exact expressions of the HPZ coefficients are related to the Green's functions of the corresponding quantum Langevin equations [58, 59]. The entanglement properties of the joint state of the oscillator and its environment have been studied in [60].

3.2. Characteristic time scales

The characteristics of the decoherence process depend on the relation between the different time scales of the systems on one hand and the decoherence time scale on the other hand. The characteristic time scales of the system — the internal system dynamics τ_s, the relaxation time scale τ_γ and the bath correlation time scale τ_b — are determined by the coefficients of the HPZ master equation (17) and can be approximated by

$$\tau_s \approx \left(\omega_0^2+\delta\Omega^2\right)^{-1/2} = \left[\omega_0^2 + \frac{\gamma\Gamma}{m}\left(1-\frac{\Gamma^2}{\omega_0^2+\Gamma^2}\right)\right]^{-1/2} \sim \omega_0^{-1}, \tag{24}$$

$$\tau_\gamma \approx \gamma_p^{-1} = \frac{m}{\gamma}\left(1+\frac{\omega_0^2}{\Gamma^2}\right) \sim \gamma^{-1}, \tag{25}$$

$$\tau_b \approx \min\{\Gamma^{-1}, \beta\hbar\} \sim \Gamma^{-1}. \tag{26}$$

The decoherence time scale τ_d for entangled coherent states is mainly governed by the phase-space separation in the form of the parameter $|\alpha|$.

3.3. Secular approximation of the HPZ master equation

Performing a secular approximation of the HPZ master equation (17) by averaging over the rapidly oscillating terms of the time-dependent coefficients (18)–(21) (which is equivalent to a rotating wave approximation after tracing over the environment without neglecting the counter-rotating terms) one gets the following approximated master equation [61–64]:

$$\dot{\rho} = -\mathrm{i}\omega_0[a^\dagger a, \rho] + \frac{\tilde{\gamma}_\downarrow(t)}{2}[2a\rho a^\dagger - a^\dagger a\rho - \rho a^\dagger a] + \frac{\tilde{\gamma}_\uparrow(t)}{2}[2a^\dagger \rho a - aa^\dagger \rho - \rho aa^\dagger]. \tag{27}$$

The form of this equation is similar to the quantum optical master equation of the damped harmonic oscillator in the Lindblad form, with the only difference that the coefficients $\tilde{\gamma}_{\downarrow,\uparrow}$ appearing in the master equation are time-dependent. The connection to the HPZ coefficients (18) and (21) is given by

$$\tilde{\gamma}_\downarrow(t) = \left(\frac{D_p(t)}{\hbar m\omega_0} + \frac{\gamma_p(t)}{2}\right) \overset{t\gg\Gamma^{-1}}{\longrightarrow} \frac{\gamma}{m}\frac{\Gamma^2}{\omega_0^2+\Gamma^2}(\bar{n}+1)\,, \tag{28}$$

$$\tilde{\gamma}_\uparrow(t) = \left(\frac{D_p(t)}{\hbar m\omega_0} - \frac{\gamma_p(t)}{2}\right) \overset{t\gg\Gamma^{-1}}{\longrightarrow} \frac{\gamma}{m}\frac{\Gamma^2}{\omega_0^2+\Gamma^2}\bar{n}. \tag{29}$$

In the limit $t \gg \Gamma^{-1}$ they reach the corresponding Markovian values adjusted by a factor $\Gamma^2/\left(\Gamma^2+\omega_0^2\right) \approx 1$. As long as the coefficients $\tilde{\gamma}_{\downarrow,\uparrow}$ are positive for all times equation (27) is of Lindblad type. However, not every master equation of the Lindblad-type form does necessarily fulfil the semigroup property [62]. For certain parameter ranges the coefficients can become negative and the dynamical evolution is of the non-Lindblad type [61].

3.4. The two-reservoir model

The dynamics of two identical, not directly interacting modes (with coordinates and momenta q_j, p_j, $j = 1, 2$) in two uncorrelated reservoirs is modeled by the interaction Hamiltonian

$$H_{\mathrm{int}} = -q_1\sum_{i=1}^{\infty} c_i x_i^b - q_2\sum_{i=1}^{\infty} c_i x_i^c \tag{30}$$

with $\left\langle x_i^b x_j^c + x_i^c x_j^b\right\rangle = 0\,\forall\, i, j$. The master equation of the reduced density matrix is then given by the sum of the master equations of two single modes [34]:

$$\dot{\rho} = \sum_{j=1}^{2}\left\{\left[\frac{p_j^2}{2i\hbar m} + \frac{m\gamma_q(t)q_j^2}{2i\hbar}, \rho\right] + \frac{\gamma_p(t)}{2i\hbar}[q_j, \{p_j, \rho\}]\right.$$
$$\left. + \frac{D_{qp}(t)}{\hbar^2}[q_j, [p_j, \rho]] - \frac{D_p(t)}{\hbar^2}[q_j, [q_j, \rho]]\right\}. \tag{31}$$

The time-dependent coefficients are given by $\gamma_q(t) = \omega_0^2 + \delta\Omega^2(t) - \gamma\Gamma/m$ and equations (18)–(21). The time evolution of a (Gaussian) two-mode squeezed state in two uncorrelated non-Markovian channels has been studied recently in [34] (while we focus on the evolution of non-Gaussian states). The authors derived a non-Markovian separability function which shows oscillations in the case of an artificial *out of resonance* bath with $\Gamma \ll \omega_0$. In this two-reservoir model the initial entanglement is always completely lost and both modes are finally uncorrelated (even at zero temperature while $\tau_1 \to \infty$). If the secular approximation is applied, the non-Markovian dynamics can be described by the master equation

$$\frac{\partial\rho}{\partial t} = \frac{\tilde{\gamma}_\downarrow(t)}{2}\sum_{j=1}^{2}\left[2a_j\rho a_j^\dagger - a_j^\dagger a_j\rho - \rho a_j^\dagger a_j\right] + \frac{\tilde{\gamma}_\uparrow(t)}{2}\sum_{j=1}^{2}\left[2a_j^\dagger\rho a_j - a_j a_j^\dagger\rho - \rho a_j a_j^\dagger\right], \tag{32}$$

with time-dependent coefficients given in equation (28). It should be noted that for $\bar{n} \to 0$ the coefficient $\tilde{\gamma}_\uparrow(t)$ is different from zero for short times and vanishes for times $t \gg \Gamma^{-1}$.

3.5. Solution of the model

In this section we present the solution of the HPZ master equation for the relevant initial states.

3.5.1. Decoherence function. Given the characteristic function $\chi_I(\eta, \nu, 0)$ of an initial preparation, the time-dependent Wigner function $W_I(q, p, t)$ can be calculated from [65]:

$$W_I(q, p, t) = \frac{1}{(2\pi\hbar)^2} \int_{-\infty}^{\infty} \mathrm{d}\eta \int_{-\infty}^{\infty} \mathrm{d}\nu \tilde{\chi}_I(\eta_t, \nu_t, 0) \exp[\mathrm{i}(\eta p + \nu q)/\hbar], \quad (33)$$

where $\tilde{\chi}_I$ is identical to the initial characteristic function by substituting $\eta_t = \dot{f}(t)\eta + \frac{1}{m} f(t)\nu$, $\nu_t = m\ddot{f}(t)\nu + \dot{f}(t)\eta$ and multiplying a Gaussian factor,

$$\tilde{\chi}_I(\eta_t, \nu_t, 0) = \chi_I\left(\dot{f}(t)\eta + \frac{1}{m} f(t)\nu, m\ddot{f}(t)\eta + \dot{f}(t)\nu; 0\right) \times \exp\left[-\frac{1}{2\hbar^2}(K_p(t)\eta^2 + 2K_{qp}(t)\eta\nu + K_q(t)\nu^2)\right]. \quad (34)$$

The coefficients $K_{p,q}(t)$ and $K_{qp}(t)$ as well as the correlations $\langle q^2(t)\rangle$, $\langle p^2(t)\rangle$ and $\langle\{q, p\}(t)\rangle$ are obtained as solution of the corresponding quantum Langevin equation with the Greens function $f(t)$. With $a = \frac{q_0}{2\sigma_0^2}\dot{f}(t)$, $b = \frac{q_0}{2m\sigma_0^2} f(t)$ and $\tilde{N}_0 = (1 + \mathrm{e}^{q_0^2/\sigma_0^2})^{-1}$ the norm $\mathrm{Tr}[\rho_I^2]$ of the interference part finally reads

$$\mu_I(t) = \mu_0(t)\tilde{N}_0 + \mu_0(t)\tilde{N}_0 \exp\left[\frac{\mu_0^2(t)q_0^2}{\hbar^2 m^2 \sigma_0^4}\left(m^2\dot{f}_t^2\langle q^2(t)\rangle - mf_t\dot{f}_t\langle\{q, p\}\rangle + f_t^2\langle p^2(t)\rangle\right)\right] \quad (35)$$

(normalized to $\mu_I(0) = 1$). This is our decoherence function.

3.5.2. Concurrence. The concurrence of a two-mode entangled coherent state under Markovian evolution in a zero-temperature environment with $\gamma_\downarrow = \gamma$ and $\gamma_\uparrow = 0$ can be calculated by introducing a time-dependent orthogonal basis,

$$|\mathbf{0}(t)\rangle \equiv |\alpha_+(t)\rangle, \qquad |\mathbf{1}(t)\rangle \equiv \frac{|\alpha_-(t)\rangle - \mathrm{e}^{-2\,\mathrm{e}^{-\gamma t}|\alpha|^2}|\alpha_+(t)\rangle}{\sqrt{1 - \mathrm{e}^{-4\,\mathrm{e}^{-\gamma t}|\alpha|^2}}} \quad (36)$$

with $|\alpha_\pm(t)\rangle = |\pm\alpha_0\,\mathrm{e}^{-\gamma t/2}\rangle$. This leads to a time-dependent density matrix $\rho_{12}(t)$ with coefficients $p(t) = \mathrm{e}^{-2\,\mathrm{e}^{-\gamma t}|\alpha|^2}$, $q(t) = \mathrm{e}^{-4(1-\mathrm{e}^{-\gamma t})|\alpha|^2}$ and $M(t) = \sqrt{1 - p^2(t)}$. Under non-Markovian evolution the constant coefficients $\gamma_\downarrow$, $\gamma_\uparrow$ have to be replaced by the time-dependent coefficients $\tilde{\gamma}_\downarrow(t)$, $\tilde{\gamma}_\uparrow(t)$ which leads to the substitution

$$\gamma t \to \Gamma_p(t) = \int_0^t \mathrm{d}s\gamma_p(s) \qquad \text{and} \qquad \Delta(t) \to \Delta_p(t) = \frac{2\,\mathrm{e}^{-\Gamma_p(t)}}{\hbar m\omega_0} \int_0^t \mathrm{d}s\,\mathrm{e}^{\Gamma_p(s)} D_p(s). \quad (37)$$

Thus, we receive the time dependent coefficients of the density matrix

$$p(t) = \mathrm{e}^{-2\,\mathrm{e}^{-\Gamma_p(t)}|\alpha|^2}, \qquad q(t) = \mathrm{e}^{-4\Delta_p(t)|\alpha|^2}, \qquad M(t) = \sqrt{1 - p^2(t)}, \quad (38)$$

From the corresponding eigenvalues $\lambda_i(t)$, $i = 1, \ldots, 4$, the concurrence can be calculated as

$$\mathcal{C}_{12}(t) = N^2 M^2(t) q(t) = \frac{1 - \mathrm{e}^{-4\,\mathrm{e}^{-\Gamma_p(t)}|\alpha|^2}}{1 - \mathrm{e}^{-4|\alpha|^2}\cos\theta}\,\mathrm{e}^{-4\Delta_p(t)|\alpha|^2}, \quad (39)$$

and should be compared to the time-dependent decoherence function of a single-mode superposition state.

4. Decoherence and disentanglement scenarios in the non-Markovian regime

4.1. Exponential and Gaussian decay

For a given system and bath parameters the decoherence time scale varies with the initial phase-space separation $|\alpha|$. The parameter $q_0 = \frac{1}{2}|q - q'|$ therefore allows us to determine the relation between the system dynamics τ_s and the decoherence timescale τ_d. In the limits $\tau_d \gg \tau_s$ and $\tau_d \ll \tau_s$ it is possible to derive approximated expressions $\mu_{\tau_d>\tau_s}(t)$ and $\mu_{\tau_d<\tau_s}(t)$ for the exact decoherence function (35) by considering just the leading terms in the HPZ master equation (17). From these approximations an explicit expression for τ_d can be obtained.

For $\tau_s \ll \tau_d \ll \tau_\gamma$ the diffusion coefficient $D_p(t)$ dominates the dynamics thus having

$$\mu_{\tau_d>\tau_s}(t) = \left(\exp\left[-2\frac{q_0^2}{\hbar^2}D_p(\infty)t\right]\right)^2 = \exp\left[-\frac{4q_0^2}{\hbar^2}\left(\int_0^\infty \mathrm{d}t' K(t')\cos\omega_0 t'\right)t\right], \tag{40}$$

where the stationary value $D_p(\infty) = \gamma_p(\infty)\langle p^2(\infty)\rangle$ with $\langle p^2(\infty)\rangle$ is received from the solution of the corresponding Langevin equation for times $t \approx \Gamma^{-1} \ll \tau_d$. For $\gamma \ll m\omega_0$ and $\Gamma \gg \omega_0$ we have $D_p(\infty) = \frac{\gamma\hbar\omega_0}{2}\coth\left(\frac{1}{2}\beta\hbar\omega_0\right)$, thus for $kT \gg \hbar\omega_0$ receiving the decoherence function

$$\mu_{\tau_d>\tau_s}(t) \overset{\gamma\ll\omega_0}{\approx} \exp\left[-\frac{4\gamma\omega_0 q_0^2}{2\hbar}\coth\left(\frac{1}{2}\beta\hbar\omega_0\right)t\right] \overset{kT\gg\hbar\omega_0}{\longrightarrow} \exp\left[-\frac{4\gamma kT q_0^2}{\hbar^2}t\right]. \tag{41}$$

Decoherence is dominated by thermal fluctuations and the decoherence function decreases exponentially with the characteristic time scale

$$\mu_{\tau_d>\tau_s}(t) \sim \exp[-t/\tau_d] \qquad \text{with} \qquad \tau_d = \frac{\hbar^2}{4\gamma kT}q_0^{-2} \tag{42}$$

and scales inverse quadratically with the displacement q_0 [66].

In the limit $\tau_d \ll \tau_s \ll \tau_\gamma$ decoherence takes place on time scales $t \ll w_0^{-1}$ and is dominated by vacuum fluctuations and system-bath interaction. The decoherence factor can be derived from influence functional path integral methods and is given by

$$\begin{aligned}\mu_{\tau_d<\tau_s}(t) &= \left(\exp\left[-\frac{4q_0^2}{\hbar^2}\int_0^t \mathrm{d}t'\int_0^{t'}\mathrm{d}t'' K(t'-t'')\right]\right)^2 \\ &= \exp\left[-\frac{8q_0^2}{\pi\hbar}\int_0^\infty \mathrm{d}\omega J(\omega)\coth\left(\frac{1}{2}\beta\hbar\omega\right)\frac{1-\cos(\omega t)}{w^2}\right].\end{aligned} \tag{43}$$

The decay of the decoherence function becomes more and more non-exponential when the parameter q_0 is increased and finally becomes Gaussian for $\tau_d \ll \tau_b \ll \tau_s \ll \tau_\gamma$ with

$$\mu_{\tau_d<\tau_s}(t) \sim \exp[-(t/\tau_d)^2] \qquad \text{with} \qquad \tau_d = \frac{\hbar}{2\sqrt{K(0)}}q_0^{-1} \overset{kT\gg\hbar\omega_0}{\longrightarrow} \frac{\hbar}{2\sqrt{\gamma\Gamma kT}}q_0^{-1}, \tag{44}$$

where the dissipation–fluctuation theorem $K(t) = kT\gamma(t) = kT\gamma\Gamma\,\mathrm{e}^{-\Gamma t}$ has been applied. In this case the decoherence time scales just linearly with the inverse initial separation q_0 and depends explicitly on the bath cut-off frequency Γ. Determining the decoherence time by just considering the diffusion term leads to an underestimation of the decoherence rate. Thus, the decoherence scenarios for mesoscopic ($\tau_s \ll \tau_d \ll \tau_\gamma$) and macroscopic separations ($\tau_d \ll \tau_s$) differ from each other [52, 67]. The different power-law scaling of τ_d with respect to the separation q_0 is illustrated in figure 1.

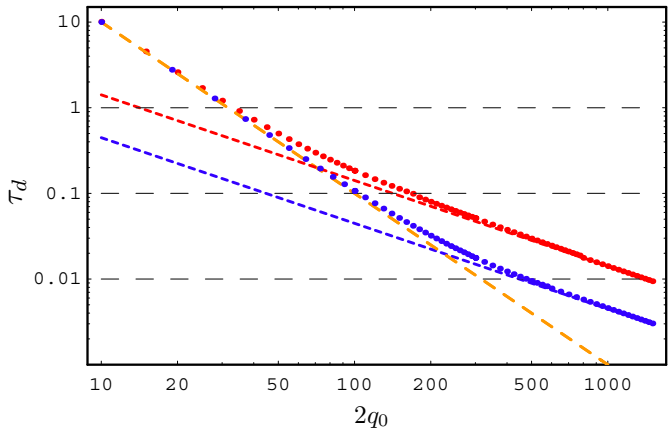

Figure 1. Decoherence time scale τ_d for $\tau_d \ll \tau_s$ at high temperatures in dependence of the separation $|q - q'| = 2q_0$. For relatively small values of q_0 and thus $\tau_d > \tau_b \approx \Gamma^{-1}$, τ_d decays according to $\hbar^2/(2\gamma kT)q_0^{-2}$ (yellow dashed). If the decoherence time becomes very small $\tau_d \ll \tau_b$, the dependence of τ_d on q_0 changes qualitatively to an inverse proportionality $\hbar/(\sqrt{\gamma\Gamma kT})q_0^{-1}$. Here: $\Gamma = 10\omega_0$ (red), $\Gamma = 100\omega_0$ (blue). Further parameters: $\gamma = 10^{-5}m\omega_0$, $kT = 50\hbar\omega_0$.

4.2. The long and short time behavior

In this section we focus on the decoherence of macroscopic superpositions (large $|\alpha|$) for the standard scenario $\tau_b \ll \tau_s \ll \tau_\gamma$ at high and low temperatures. The decoherence time scale τ_d thus has the same magnitude as the internal system dynamics τ_s. In this case the functions (40) and (43) are still useful as limiting cases of (35) for short times $t \ll \tau_s$ and long times $t \gg \tau_s$ respectively, since

$$\text{for} \quad \tau_d \approx \tau_s: \qquad \mu_I(t) \approx \begin{cases} \mu_{\tau_d<\tau_s}(t) & \text{for} \quad 0 < t < \tau_1, \quad \text{where} \quad \tau_1 \ll \tau_d, \\ \mu_{\tau_d>\tau_s}(t) & \text{for} \quad \tau_2 < t < \infty, \quad \text{where} \quad \tau_2 \gg \tau_d. \end{cases} \tag{45}$$

However, in the intermediate region $t \approx \tau_s \approx \tau_d$ the time evolution of $\mu_I(t)$ is different from these approximations. Thus, an explicit expression for τ_d cannot be derived. Nevertheless further insights into the short and long time behavior are gained by considering the low and high temperature limits respectively.

For $kT \gg \hbar\omega_0$ the functions (40) and (43) become

$$\mu_{\tau_d>\tau_s}(t) = \mathrm{e}^{-(4\gamma kTq_0^2/\hbar^2)t} \qquad \text{and} \qquad \mu_{\tau_d<\tau_s}(t) = \mathrm{e}^{-(8\gamma kTq_0^2/\hbar^2)t}. \tag{46}$$

These approximated functions decay exponentially and differ just by a factor of two in the exponent. From figure 2(*a*) one can see that the decoherence function (35) follows the function $\mu_{\tau_d<\tau_s}(t)$ for short times $t < \tau_s$ and for large times $t \gg \tau_s$ oscillates around the approximation $\mu_{\tau_d>\tau_s}(t)$. The oscillations result from the rotation and *breathing* of the Wigner function in phase space (with frequency $\omega_0 \sim \tau_s^{-1}$) which is connected to a periodical change between superposition in coordinate and momentum space. For low temperatures $kT \ll \hbar\omega_0$ the functions (40) and (43) become

$$\mu_{\tau_d>\tau_s}(t) = \mathrm{e}^{-(2\gamma\omega_0q_0^2/\hbar)t} \qquad \text{and} \qquad \mu_{\tau_d<\tau_s}(t) \sim \begin{cases} \mathrm{e}^{-\frac{8\gamma\Gamma^2q_0^2}{\pi\hbar}t^2} & \text{for} \quad t \ll \tau_s, \\ t^{-\frac{8\gamma q_0^2}{\hbar\pi}} & \text{for} \quad t \gg \tau_s. \end{cases} \tag{47}$$

Figure 2(*b*) shows that the decoherence function (35) for short times $t < \tau_s$ decays fast in accordance with the evolution of $\mu_{\tau_d<\tau_s}(t)$, while the long-time behavior for $t \gg \tau_s$ is

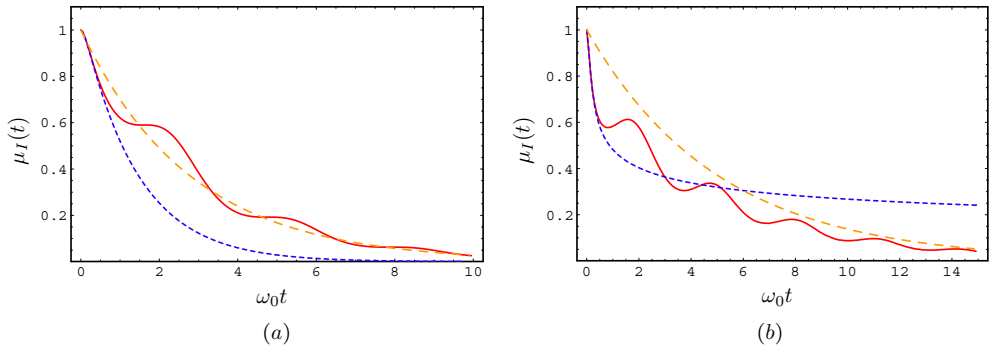

Figure 2. Time evolution of the decoherence function (35) (red line) in comparison to the approximation (43) (blue dashed line) and (40) (yellow dashed line) for high temperatures (*a*) and low temperatures (*b*). The oscillations result from the rotation and *breathing* of the Wigner function in phase space (with frequency $\omega_0 \sim \tau_s^{-1}$) which is related to a periodical change between superpositions in coordinate and momentum space. Further parameters: $\gamma = 10^{-5}\omega_0$, $\Gamma = 10\omega_0$. (*a*) $kT = 10\hbar\omega_0$, $|\alpha_0|^2 = 30$. (*b*) $kT = 10^{-3}\hbar\omega_0$, $|\alpha_0|^2 = 100$.

again well approximated by $\mu_{\tau_d>\tau_s}(t)$. The long-time behavior of $\mu_{\tau_d<\tau_s}(t)$ however can be characterized by a power law decay $\sim t^{-\gamma q_0^2}$. This result is in accordance with the behavior of a free quantum Brownian particle [68]. There is no longer characteristic decoherence time. In our case the decoherence function follows an algebraic decay for intermediate times and an exponential decay for large times.

4.3. Numerical analysis of the dynamics

4.3.1. Decoherence of a single-mode superposition. Describing decoherence processes within the Born–Markov approximation is valid as long as the time scale of bath correlations τ_b is the smallest time scale. Since the decoherence time scale τ_d is inversely proportional to the bath temperature T and to the squared separation q_0^2, the decoherence process takes place on time scales that are comparable to the bath correlation time. In this case, non-Markovian influences become important.

A gradual change from the Markovian to the non-Markovian regime can be studied by varying the bath correlation time in the form of the inverse cutoff frequency Γ^{-1} and the decoherence time scale τ_d by the parameter $|\alpha_0| = q_0/2\sigma_0$. Such a change from the Markovian ($\tau_d \gg \tau_b$) to the non-Markovian regime ($\tau_d \ll \tau_b$) is illustrated in figures 3(*a*)–(*f*) by the evolution of $\mu_I(t)$, $\mu_{\tau_d>\tau_s}(t)$ and $\mu_{\tau_d<\tau_s}(t)$. Figures 3(*a*)–(*c*) show that a reduction of Γ slows down the decoherence process. For example, the decoherence time in figure 3(*c*) for $\Gamma = 2\omega_0$ is five times larger than the decoherence time in figure 3(*a*) for $\Gamma = 100\omega_0$. More important are the qualitative changes in the evolution of the three decoherence measures $\mu_I(t)$, $\mu_{\tau_d>\tau_s}(t)$ and $\mu_{\tau_d<\tau_s}(t)$. In figures 3(*a*)–(*d*) the norm $\mu_I(t)$ follows $\mu_{\tau_d<\tau_s}(t)$, since the decoherence time is smaller than the characteristic system time scale $\tau_s \sim \omega_0^{-1}$. A comparison to the case $\tau_d \gg \tau_s$ is shown in figure 3(*d*) where $\mu_I(t)$ follows the evolution of $\mu_{\tau_d>\tau_s}(t)$.

So far, we have considered non-Markovian influences by approaching τ_d and τ_b, where the limiting cases for $\tau_d \gg \tau_s$ and $\tau_d \ll \tau_s$ have been distinguished. A further distinctive feature can be observed if additionally the condition $\tau_b \gg \tau_s$ is fulfilled which means $\omega_0 \gg \Gamma$. In this case the bath could be characterized as *out-of-resonance* [61]. The relaxation timescale $\tau_\gamma \sim \gamma\omega_0^2/\Gamma^2$ also depends on the cut-off frequency but still remains by far the largest time

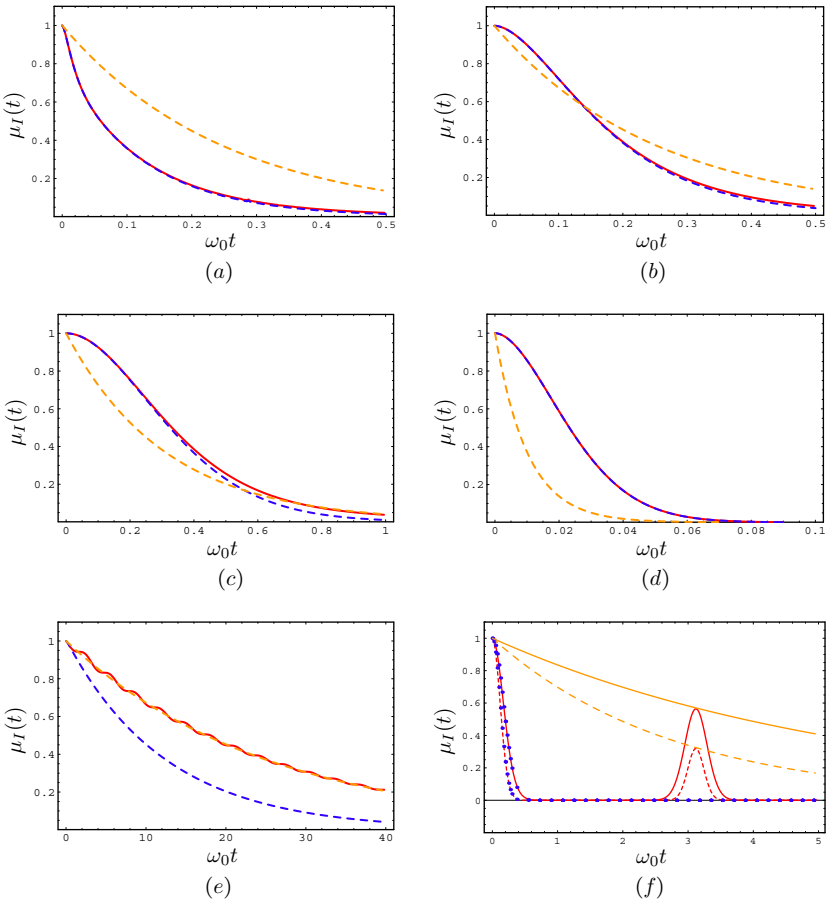

Figure 3. Time evolution of the decoherence function (35) (red lines) in comparison to the approximation (43) (blue lines) and (40) (yellow lines) at high temperature $kT = 10\hbar\omega_0$ and small coupling $\gamma = 10^{-5}\omega_0$ in (a)–(e). Figures (a)–(d) illustrate the transition from the Markovian ($\tau_d \gg \tau_b$) to the non-Markovian regime ($\tau_d \ll \tau_b$), related to the ratio of decoherence time τ_d and bath correlation time scale $\tau_b \approx \Gamma^{-1}$. The decoherence function $\mu_I(t)$ follows the approximated function (43) since $\tau_d \ll \tau_s \sim \omega_0^{-1}$. A comparison with the case $\tau_d \gg \tau_s$, where $\mu_I(t)$ follows the function (40) is plotted in figure (e). Figure (f) illustrates the partial revivals of coherence in an out-of-resonance-bath. (a) $\tau_d \gg \tau_b$ for $\Gamma = 100\omega_0$, $|\alpha_0| = 100$. (b) $\tau_d \approx \tau_b$ for $\Gamma = 10\omega_0$, $|\alpha_0| = 100$. (c) $\tau_d \approx \tau_b$ for $\Gamma = 2\omega_0$, $|\alpha_0| = 100$. (d) $\tau_d < \tau_b$ for $\Gamma = 10\omega_0$, $|\alpha_0| = 500$. (e) $\tau_b \ll \tau_s \ll \tau_d$ for $\Gamma = 10\omega_0$, $|\alpha_0| = 10$. (f) $\tau_b \gg \tau_s$ for $\Gamma = 0.01\omega_0$, $|\alpha_0| = 30$ and $\gamma = 0.05\omega_0$ compared to $\gamma = 0.1\omega_0$ (dashed lines).

scale. The time evolution of the decoherence function $\mu_I(t)$ cannot be well approximated by $\mu_{\tau_d<\tau_s}$ or $\mu_{\tau_d>\tau_s}$ alone. Figure 3(f) shows an example. For short times the norm $\mu_I(t)$ decays very fast, following the approximated function $\mu_{\tau_d<\tau_s}$. However, within the half of a system period $\omega_0 t \approx \pi$ a partial revival of coherence takes place and the function $\mu_I(t)$ reaches a relative maximum that is given by the corresponding value of the limit case $\mu_{\tau_d>\tau_s}$. Although the characteristic time scales of $\mu_{\tau_d<\tau_s}$ and $\mu_{\tau_d>\tau_s}$ are quite different, only both limit cases taken together give an accurate picture of the decoherence process in this regime. The corresponding master equation (27) in this case is not of Lindblad type with partially negative values of the coefficients $\tilde{\gamma}_\uparrow(t)$ and $\tilde{\gamma}_\downarrow(t)$.

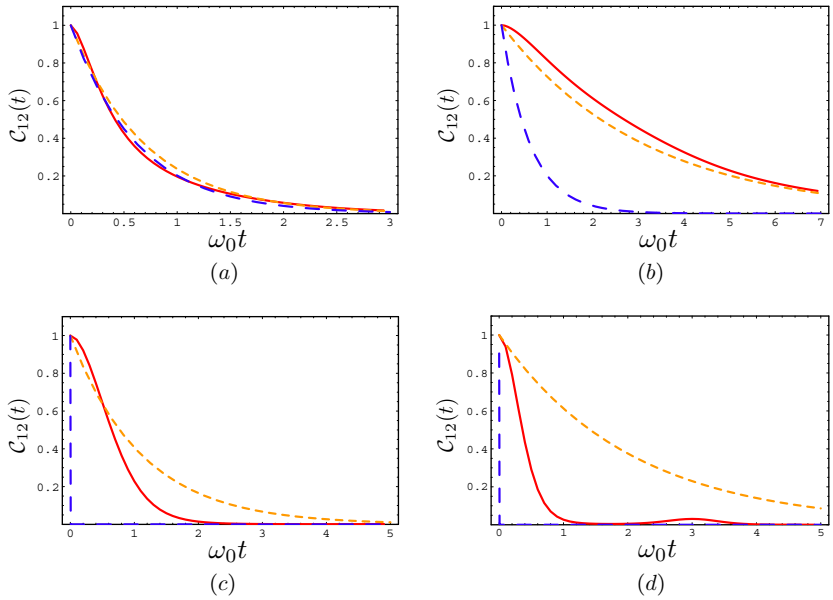

Figure 4. Time evolution of the concurrence $C_{12}(t)$ (red line) for a two-mode entangled coherent state $|\Phi_+\rangle = |\alpha, \theta = 0, N = 2\rangle$ in a zero-temperature environment with small ratios Γ/ω_0 and $\gamma = 10^{-3}\omega_0^2$. In comparison the Markovian evolution is plotted for relaxation time γ^{-1} (blue line) and with adjusted relaxation time τ_γ (yellow dashed line). In a moderate non-Markovian regime the entanglement is preserved for longer times (*b*) while it is lost faster in an out-of-resonance bath with $\Gamma \ll \omega_0$ (*c*). The behavior of the concurrence is similar to that of the decoherence function. Revivals can occur even at zero temperature (*d*). (*a*) $\Gamma = 3\omega_0, |\alpha_0| = 20$. (*b*) $\Gamma = 0.5\omega_0, |\alpha_0| = 20$. (*c*) $\Gamma = 10^{-2}\omega_0, |\alpha_0| = 1500$. (*d*) $\Gamma = 10^{-3}\omega_0, \gamma = 10^{-2}\omega_0^2, |\alpha_0| = 3500$.

4.3.2. Disentanglement of a two-mode entangled coherent state. In the following, we compare the findings on the decoherence process of a single-mode superposition state to the behavior of the concurrence of a two-mode entangled coherent state. Figures 4(*a*)–(*d*) show the time evolution of the concurrence $C_{12}(t)$ of an entangled coherent state $|\Phi_+\rangle = |\alpha, \theta = 0, N = 2\rangle$ in reservoirs with different specification of their non-Markovian character in the form of the relation Γ/ω_0. Qualitatively the time evolution resembles strongly the results for a single-mode superposition cat state. Starting from a quasi-Ohmic bath with ($\Gamma \gg \omega_0$) in figure 4(*a*) a reduction of the cut-off frequency leads to deviations between the Markovian and non-Markovian results. For moderate non-Markovian influences the entanglement is preserved most efficiently (figure 4(*b*)). In the strongly non-Markovian out-of-resonance bath with $\Gamma < \omega_0$ this relation is only valid at short times while for longer times the non-Markovian concurrence even decays faster, as can be seen from figure 4(*c*). The occurrence of coherence revivals is similar to the results found for the decoherence function of a single-mode superposition of coherent states.

5. Summary and conclusions

In this paper we have analyzed the non-Markovian effects on decoherence and disentanglement processes of non-Gaussian continuous variable systems within the quantum Brownian motion

model. We have compared the time evolution of the decoherence function of a single-mode cat state with the evolution of the concurrence of a two-mode entangled coherent state. For both cases, separately, we studied different decoherence and disentanglement scenarios depending on the relation between the characteristic time scales of system and environment. We found exponential, Gaussian and algebraic decay patterns of the decoherence function in the moderate non-Markovian regime and revivals of decoherence and concurrence in strongly non-Markovian out-of-resonance reservoirs.

References

[1] Braunstein S L and Pati A K 2003 *Quantum Information Theory with Continuous Variables* (Dordrecht: Kluwer)
[2] Braunstein S and van Look P 2005 *Rev. Mod. Phys.* **77** 513
[3] Cerf N J, Leuchs G and Polzik E S 2007 *Quantum Information with Continuous Variables of Atoms and Light* (London: Imperial College Press)
[4] Furusawa A, Sorensen J L, Braunstein S L, Fuchs C A, Kimble H J and Polzik E S 1998 *Science* **282** 706
[5] Braunstein S L and Kimble H J 1998 *Phys. Rev. Lett.* **80** 869
[6] Simon R 2000 *Phys. Rev. Lett.* **84** 2726
[7] Duan L M, Giedke G, Cirac J I and Zoller P 2000 *Phys. Rev. Lett.* **84** 2722
[8] Vidal G and Werner R F 2002 *Phys. Rev.* A **65** 032314
[9] Giedke G, Wolf M M, Krüger O, Werner R F and Cirac J I 2003 *Phys. Rev. Lett.* **91** 107901
[10] Zeh H D 1970 *Found. Phys.* **1** 69
[11] Zeh H D 1973 *Found. Phys.* **3** 109
[12] Zurek W H 1981 *Phys. Rev.* D **24** 1516
[13] Schlosshauer M 2004 *Rev. Mod. Phys.* **76** 1267
[14] Zurek W H 2003 *Rev. Mod. Phys.* **75** 715
[15] Joos E, Zeh H D, Kiefer C, Guilini D, Kupsch J and Stamatescu I O 2003 *Decoherence and the Appearance of a Classical World in Quantum Theory* (Berlin: Springer)
[16] Bolivar A O 2004 *Quantum-Classical Correspondance. Dynamical Quantization and the Classical Limit* (Berlin: Springer)
[17] Halliwell J J, Perez-Mercader J and Zurek W H 1994 *Physical Origins of Time Asymmetry* (Cambrige: Cambrige University Press)
[18] Zeh H D 1999 *The Physical Basis of the Direction of Time* (Singapur: Springer)
[19] Breuer H P and Petruccione F 2003 *The Theory of Open Quantum Systems* (Oxford: Oxford University Press)
[20] Dittrich T, Hänggi P, Ingold G L, Kramer B, Schön G and Zwerger W 1998 *Quantum Transport and Dissipation* (Weinheim: Wiley-VCH)
[21] Prauzner-Bechcicki J S 2004 *J. Phys. A: Math. Gen.* **37** L173
[22] Braun D 2002 *Phys. Rev. Lett.* **89** 277901
[23] Olivares S, Paris M G A and Rossi A R 2003 *Phys. Lett.* A **319** 32
[24] Serafini A, Illuminati F, Paris G A M and De Siena S 2004 *Phys. Rev.* A **69** 022318
[25] Kim M S, Lee J, Ahn D and Knight P L 2002 *Phys. Rev.* A **65** 040101
[26] Yi X X, Yu C S, Zhou L and Song H S 2003 *Phys. Rev.* A **68** 052304
[27] Plenio M B and Huelga S F 2002 *Phys. Rev. Lett.* **88** 197901
[28] Benatti F and Floreanini R 2006 *J. Phys. A: Math. Gen.* **39** 2689
[29] Benatti F and Floreanini R 2006 *Int. J. Quant. Inf.* **4** 395
[30] Rajagopal A K and Rendell R W 2001 *Phys. Rev.* A **63** 022116
[31] Walls D F and Milburn G J 1994 *Quantum Optics* (Berlin: Springer)
[32] Ban M 2006 *J. Phys. A: Math. Gen.* **39** 1927
[33] McAneney H, Lee J, Ahn D and Kim M S 2005 *J. Mod. Opt.* **52** 935
[34] Maniscalco S, Olivares S and Paris M G A 2007 *Phys. Rev.* A **75** 062119
[35] An J H, Feng M and Zhang W M 2007 *Preprint* arXiv:0705.2472
[36] Liu K L and Goan H S 2007 *Preprint* arXiv:0706.0996
[37] An J H and Zhang W M 2007 *Preprint* arXiv:0707.2278
[38] Caldeira A O and Leggett A J 1983 *Physica* A **121** 587
[39] Ford G W, Lewis J T and O'Connell R F 1988 *J. Stat. Phys.* **53** 439
[40] Hu B L, Paz J P and Zhang Y 1992 *Phys. Rev.* D **45** 2843
[41] Sanders B C 1992 *Phys. Rev.* A **45** 6811

[42] Wang X and Sanders B C 2001 *Phys. Rev.* A **65** 012303
[43] Hirota O and Sasaki M 2001 *Preprint* quant-ph/0101018
[44] Hirota O, van Enk J S, Nakamura K, Sohma M and Kentaro K 2001 *Preprint* quant-ph/0101018
[45] Mann A, Sanders B C and Munro W J 1995 *Phys. Rev.* A **51** 989
[46] Chai C L 1992 *Phys. Rev.* A **1992** 7187
[47] Tan S M, Walls D F and Collett M J 1991 *Phys. Rev. Lett.* **66** 252
[48] Wang X 2002 *J. Phys. A: Math. Gen.* **35** 165
[49] van Enk S J and Hirota O 2001 *Phys. Rev.* A **64** 022313
[50] van Enk S J and Hirota O 2005 *Phys. Rev.* A **71** 062322
[51] Li S B and Xu J B 2003 *Phys. Lett.* A **309** 321
[52] Strunz W T, Haake F and Braun D 2003 *Phys. Rev.* A **67** 022101
[53] Hill S and Wootters K W 1997 *Phys. Rev. Lett.* **78** 5022
[54] Wootters W K 1998 *Phys. Rev. Lett.* **80** 2245
[55] Caldeira A O and Leggett A J 1983 *Ann. Phys., NY* **149** 374
[56] Caldeira A O and Leggett A J 1981 *Phys. Rev. Lett.* **46** 211
[57] Ford G W, Kac M and Mazur P 1965 *J. Math. Phys.* **6** 504
[58] Karrlein R and Grabert H 1997 *Phys. Rev.* E **55** 153
[59] Haake F and Reibold R 1985 *Phys. Rev.* A **32** 2462
[60] Eisert J and Plenio M B 2002 *Phys. Rev. Lett.* **89** 137902
[61] Maniscalco S, Piilo J, Intravaia F, Petruccione F and Messina A 2004 *Phys. Rev.* A **70** 032113
[62] Intravaia F, Maniscalco S and Messina A 2003 *Phys. Rev.* A **67** 042108
[63] Intravaia F, Maniscalco S, Piilo J and Messina A 2003 *Phys. Lett.* A **308** 6
[64] Maniscalco S, Piilo J, Intravaia F, Petruccione F and Messina A 2004 *Phys. Rev.* A **69** 052101
[65] Ford G W and O'Connell R F 2001 *Phys. Rev.* D **64** 105020
[66] Walls D F and Milburn G J 1985 *Phys. Rev.* A **31** 1059
[67] Strunz W T and Haake F 2003 *Phys. Rev.* A **67** 022102
[68] Sinha S 1997 *Phys. Lett.* A **228** 1